

Ocean Turbulence. Part I: One-Point Closure Model—Momentum and Heat Vertical Diffusivities

V. M. CANUTO,* A. HOWARD, Y. CHENG, AND M. S. DUBOVIKOV

NASA Goddard Institute for Space Studies, New York, New York

(Manuscript received 9 September 1999, in final form 7 July 2000)

ABSTRACT

Ocean mixing processes have traditionally been formulated using one-point turbulence closure models, specifically the Mellor and Yamada (MY) models, which were pioneered in geophysics using 1980 state-of-the-art turbulence modeling. These models have been widely applied over the years, but the underlying core physical assumptions have hardly improved since the 1980s; yet, in the meantime, turbulence modeling has made sufficient progress to allow four improvements to be made.

- 1) *The value of Ri_{cr} .* MY-type models yield a low value for the critical Richardson number, $Ri_{cr} = 0.2$ (the result of linear stability is $Ri_{cr} = 1/4$). On the other hand, nonlinear stability analysis, laboratory measurements, direct numerical simulation, large eddy simulation, and mixed layer studies indicate that $Ri_{cr} \sim 1$. The authors show that by improving the closure for the pressure correlations, the result $Ri_{cr} \sim 1$ naturally follows.
- 2) *Nonlocal, third-order moments (TOMs).* The downgradient approximation used in all models thus far seriously underestimates the TOMs. A new expression that includes both stratification and shear is presented here for the first time. It is obtained by solving the dynamic equations for the third-order moments.
- 3) *Rotation.* The MY-type models with rotation assume that the latter does not affect turbulence, specifically, neither the pressure correlations nor the rate of dissipation of turbulent kinetic energy. Recent studies show that both quantities are affected.
- 4) *Mixing below the mixed layer.* Thus far, the momentum and heat diffusivities below the mixed layer have been treated as adjustable parameters. A new model that allows use of the same turbulence model throughout the ocean depth is proposed.

A new model is presented that includes 1), 2), and 4). Rotation will be dealt with in a subsequent paper. The new model is fully algebraic and easy to use in an ocean code. The new model is used in an OGCM, and the predicted global temperature and salinity profiles are compared with those of the KPP model and Levitus data.

1. Introduction

When solving an ocean model one solves the equations for the mean variables, that is, the mean velocity U and the mean temperature T . Using the standard notation $D/Dt \equiv \partial/\partial t + U_i \partial/\partial x_i$, $\lambda_i = g_i \alpha$, $g_i = (0, 0, g)$, where α is the volume expansion coefficient, the dynamic equations for U and T are ($a_{,i} \equiv \partial a/\partial x_i$, $a_{,ij} \equiv \partial a_i/\partial x_j$):

$$DU_i/Dt = -(g_i + \rho^{-1} P_{,i}) - \tau_{ij,j} \quad (1a)$$

$$DT/Dt = -h_{,i} + (c_p \rho)^{-1} I_{,z}, \quad (1b)$$

where I is the solar radiation flux. Turbulence enters through the Reynolds stress tensor τ_{ij} and the heat flux h_i , which are defined as

$$\tau_{ij} = \overline{u_i u_j}, \quad h_i = \overline{u_i \theta}, \quad (1c)$$

where u_i and θ are the fluctuating components of the velocity and temperature fields and where the overbar indicates an ensemble average. Using a well-known procedure, it is a matter of algebra, not physics, to derive the dynamic equations for the variables (1c) (Chou 1940, 1945; Lumley and Khajeh-Nouri 1974; Launder et al. 1975; Pope 1975; Lumley 1978; Rodi 1976; Shih and Shabbir 1992; Gatski et al. 1992; Canuto 1994). Thus, we present such equations without derivation. The reliability of any model is predicated upon the physical content of its ingredients, which we shall try to improve vis-à-vis previous models. We have

Reynolds stresses τ_{ij} :

$$\begin{aligned} \frac{D}{Dt} \tau_{ij} + D_f(\tau_{ij}) = & -\tau_{jk} U_{i,k} - \tau_{ik} U_{j,k} + \lambda_i h_j \\ & + \lambda_j h_i - \Pi_{ij} - \frac{2}{3} \epsilon \delta_{ij}, \end{aligned} \quad (2a)$$

where

* Additional affiliation: Department of Applied Physics, Columbia University, New York, New York.

Corresponding author address: Dr. Vittorio M. Canuto, NASA Goddard Institute for Space Studies, 2880 Broadway, New York, NY 10025.

E-mail: acvmc@giss.nasa.gov

$$D_f(\tau_{ij}) \equiv \frac{\partial}{\partial x_k} (\overline{u_i u_j u_k}), \quad \Pi_{ij} \equiv \overline{u_i p_{,j}} + \overline{u_j p_{,i}} \quad (2b)$$

Heat flux h_i :

$$\frac{D}{Dt} h_i + D_f(h_i) = -\tau_{ij} T_{,j} - h_j U_{i,j} + \lambda_i \overline{\theta^2} - \Pi_i^\theta, \quad (3a)$$

where

$$D_f(h_i) = \frac{\partial}{\partial x_j} (\overline{\theta u_i u_j}), \quad \Pi_i^\theta \equiv \overline{\theta p_{,i}} \quad (3b)$$

Temperature variance $\overline{\theta^2}$:

$$\frac{D\overline{\theta^2}}{Dt} + D_f(\overline{\theta^2}) = -2h_i T_{,i} - 2\epsilon_\theta, \quad (4a)$$

where

$$D_f(\overline{\theta^2}) \equiv \frac{\partial}{\partial x_i} (\overline{u_i \theta^2}) \quad (4b)$$

Turbulent kinetic energy $K \equiv 1/2 \tau_{ii}$:

$$\frac{DK}{Dt} + D_f(K) = -\tau_{ij} U_{i,j} + \lambda_i \overline{u_i \theta} - \frac{1}{2} \Pi_{ii} - \epsilon \quad (5a)$$

$$D_f(K) \equiv \frac{\partial}{\partial x_i} \left(\frac{1}{2} \overline{q^2 u_i} \right), \quad q^2 \equiv u_i u_i \quad (5b)$$

Dissipation rate of turbulent kinetic energy, ϵ

$$\frac{D\epsilon}{Dt} + D_f(\epsilon) = (P - c_2 \epsilon) \epsilon K^{-1} + c_s |N| \epsilon \quad (5c)$$

$$D_f(\epsilon) \equiv \frac{\partial}{\partial x_i} (\overline{\epsilon u_i}), \quad P_s = -\tau_{ij} S_{ij}, \quad (5d)$$

$$P_b = \alpha g_i h_i$$

Here $P \equiv c_1 P_s + c_3 P_b$ is the total production due to buoyancy and shear. Dissipation of potential energy, ϵ_θ :

$$\epsilon_\theta = \tau_\theta^{-1} \overline{\theta^2} \quad (5e)$$

Let us now discuss each equation in turn. The first four terms on the right-hand side of (2a) represent the sources and sinks of τ_{ij} due to shear and stratification and they present no closure problems. The difficulties lie in the terms D_f , Π_{ij} , and ϵ . The first represents the diffusion of Reynolds stresses, and from the definition in (2b) one sees that it entails higher-order moments, specifically the third-order moments (TOMs). This is the first closure problem. The terms Π_{ij} represent the contribution of pressure forces. Since pressure is an energy, Π_{ij} is a third-order moment that needs closure. Finally, ϵ is rate of dissipation of τ_{ij} due to viscous forces and also needs closure. The same general considerations hold true for Eq. (3a), where the first three terms present no closure problems, whereas the diffusion term D_f and the pressure correlation term Π_i^θ must be expressed in terms of the other variables in order for the equation to be solved. The same difficulties arise in trying to solve

Eq. (4a) for the potential energy, where one must know the diffusion term D_f and the rate of dissipation of potential energy ϵ_θ . Finally, Eq. (5e) has been widely used over the years, as discussed in the literature cited after Eq. (1c) above. Once substituted in (4a), it amounts to finding the dissipation timescale τ_θ . For many years, the relation $\tau_\theta = c\tau$ was used and the coefficient c determined on a specific flow. Recent theoretical work (Canuto and Dubovikov 1996a) has allowed for the determination of the function τ_θ versus τ , as discussed in section 6, where we also discuss the coefficients in Eq. (5c).

In summary, the full problem demands (i) a closure for the pressure correlation terms, (ii) the effect of rotation, (iii) a closure for the TOM, and (iv) the effect of rotation on the dissipation terms. We have developed a new model that includes (i)–(iv), but due to space limitations, here we discuss only topics (i) and (iii), while (ii) and (iv) will be dealt with in a subsequent paper.

2. Pressure correlations

The literature on this topic is quite extensive (Lumley and Khajeh-Nouri 1974; Launder et al. 1975; Pope 1975; Lumley 1978; Rodi 1976; Shih and Shabbir 1992; Gatski et al. 1992). We only recall that it is generally agreed that the tensor Π_{ij} contains three terms: the return to isotropy (Rotta term or slow part), the mean shear interaction (rapid part), and the buoyancy contribution. They are expressed as

$$\Pi_{ij} = 2\tau_{pv}^{-1} b_{ij} - \frac{4}{5} K S_{ij} + (1 - \beta_5) B_{ij}, \quad (6a)$$

where

$$b_{ij} = \tau_{ij} - \frac{2}{3} K \delta_{ij}, \quad S_{ij} = \frac{1}{2} (U_{i,j} + U_{j,i}),$$

$$B_{ij} = \lambda_i h_j + \lambda_j h_i - \frac{2}{3} \delta_{ij} \lambda_k h_k. \quad (6b)$$

Equation (6a) is, however, not complete since one can notice that vorticity V_{ij} is missing in (6a), which is not justified since shear and vorticity are two independent tensors and both should be present. However, since V_{ij} is antisymmetric while Π_{ij} is symmetric, one cannot simply add a term like the second term in (6a) with V_{ij} instead of S_{ij} . One must first construct a symmetric tensor using V_{ij} and b_{ij} and then add it to (6a). The simplest such (traceless) term is

$$Z_{ij} = V_{ik} b_{kj} + V_{jk} b_{ik}, \quad 2V_{ij} = U_{i,j} - U_{j,i}. \quad (6c)$$

There is an additional problem: There is no reason a priori why all the terms on the right-hand side of (6a), which we can call “production” of pressure correlations, should be “aligned” with Π_{ij} as the terms in (6a) are. It has, in fact, been found that one must also have

an ‘‘anisotropic production’’ term that can clearly be contributed only by the shear. The simplest such (traceless) term is of a form analogous to (6c),

$$\Sigma_{ij} = S_{ik}b_{kj} + S_{jk}b_{ik} - \frac{2}{3}\delta_{ij}S_{kl}b_{kl}. \quad (6d)$$

Adding the two new terms (6c,d) to (6a) leads to the general form for Π_{ij} :

$$\begin{aligned} \Pi_{ij} = & 2\tau_{pv}^{-1}b_{ij} - \frac{4}{5}KS_{ij} + (1 - \beta_5)B_{ij} - \alpha_1\Sigma_{ij} \\ & - \alpha_2Z_{ij}. \end{aligned} \quad (7a)$$

The ratio τ_{pv}/τ (pressure–velocity), β_5 , and $\alpha_{1,2}$ will be discussed in section 6.

The Mellor and Yamada (1982; Mellor 1989) and Kantha and Clayson (1994) models use

$$\Pi_{ij} = 2\tau_{pv}^{-1}b_{ij} - \frac{4}{5}KS_{ij}, \quad (7b)$$

which lacks buoyancy, anisotropic production, and vorticity contribution.

An analogous problem arises with the other pressure correlation Π_i^θ . Using general arguments like the preceding ones, one obtains the general form

$$\Pi_i^\theta = \tau_{p\theta}^{-1}h_i + \gamma_1\lambda_i\overline{\theta^2} - \frac{3}{4}\alpha_3\left(S_{ij} + \frac{5}{3}V_{ij}\right)h_j, \quad (7c)$$

where γ_1 and α_3 are constants and so is the ratio $\tau_{p\theta}/\tau$. The MY and D’Alessio et al. (1998) models take

$$\Pi_i^\theta = \tau_{p\theta}^{-1}h_i, \quad \Pi_i^\theta = \tau_{p\theta}^{-1}h_i + \gamma_1\lambda_i\overline{\theta^2}, \quad (7d)$$

which are incomplete vis-à-vis (7c). In the present work, we adopt the general expressions (7a) and (7c). As we shall show, the inclusion of buoyancy, shear, and vorticity has the consequence of changing the MY-type models prediction, $Ri_{cr} = 0.2$ to $Ri_{cr} \approx 1$.

3. Third-order moments (TOMs)

The diffusion terms D_f appearing in Eqs. (2)–(5), which entail third-order moments, physically represent the nonlocal character of turbulence. The prototype is the flux of turbulent kinetic energy appearing in Eq. (5b). The physical meaning of this term is as follows. Even if there were no external forces and the right-hand side of (5a) were negative (e.g., one can imagine a situation with negligible shear and stable stratification), Eq. (5a) could still be balanced since $D_f(K)$ may act as a source of turbulent kinetic energy that is not produced locally but diffused from other regions. The most widely used expression for $D_f(K)$ is the so-called downgradient approximation (DGA):

$$\begin{aligned} D_f(K) &= \frac{\partial}{\partial z}F(K), \quad F(K) = \frac{1}{2}\overline{q^2w}, \\ F(K) &= -K_m\frac{\partial K}{\partial z}, \end{aligned} \quad (8a)$$

where K_m is the momentum diffusivity that must be specified. The third equation of (8a) predicts regions of negative $F(K)$, contrary to what is observed in the PBL (Canuto et al. 1994). Furthermore, Moeng and Wyngaard (1989) have shown that the DGA severely underestimates (up to a factor of ~ 30) the true value of the TOM. However, all ocean turbulence models thus far that employ a prognostic equation for K have adopted (8a) (Rosati and Miyakoda 1988; Galperin et al. 1988; Gaspar et al. 1990; Baum and Caponi 1992; Blanke and Delecluse 1993; Ma et al. 1994; Kantha and Clayson 1994; Burchard and Baumert 1995; D’Alessio et al. 1998).

Once the downgradient approximation is abandoned, the only alternative is to consider the dynamic equations for the third-order moments (Canuto 1992):

$$\begin{aligned} & \left(\frac{D}{Dt} + \tau_3^{-1}\right)\overline{u_i u_j u_k} \\ &= -(\overline{u_i u_j u_k} U_{k,l} + \text{perm}) - (\tau_{ij}\tau_{jkl} + \text{perm}) \\ &+ (1 - c_{11})(\lambda_i\overline{\theta u_j u_k} + \text{perm}) \\ &- \frac{2}{3\tau}(\delta_{ij}\overline{q^2 u_k} + \text{perm}) \end{aligned} \quad (8b)$$

$$\begin{aligned} & \left(\frac{D}{Dt} + \tau_3^{-1}\right)\overline{u_i u_j \theta} \\ &= \overline{u_i u_j u_k} \beta_k - (\overline{u_i u_k \theta} U_{j,k} + \overline{u_j u_k \theta} U_{i,k}) \\ &- (\tau_{ik}h_{j,k} + \tau_{jk}h_{i,k} + h_k\tau_{ijk}) + \frac{2}{3}c_{11}\delta_{ij}\lambda_k\overline{\theta^2 u_k} \\ &+ (1 - c_{11})(\lambda_i\overline{\theta^2 u_j} + \lambda_j\overline{\theta^2 u_i}) \end{aligned} \quad (8c)$$

$$\begin{aligned} & \left(\frac{D}{Dt} + \tau_3^{-1} + 2\tau_\theta^{-1}\right)\overline{u_i \theta^2} \\ &= 2\beta_j\overline{\theta u_i u_j} - \overline{\theta^2 u_j} U_{i,j} - 2h_j\frac{\partial h_i}{\partial x_j} \\ &+ (1 - c_{11})\lambda_i\overline{\theta^3} - \tau_{ij}\frac{\partial}{\partial x_j}\overline{\theta^2} \end{aligned} \quad (8d)$$

$$\left(\frac{D}{Dt} + \frac{c_{10}}{c_8}\tau_3^{-1}\right)\overline{\theta^3} = 3\beta_j\overline{\theta^2 u_j} - 3h_j\frac{\partial}{\partial x_j}\overline{\theta^2}. \quad (8e)$$

Here $\beta_i \equiv -\partial T/\partial x_i$, $\tau_3 \equiv \tau/2c_8$ and perm means the one must add the terms with the (not dummy) indices permuted; the values of the constants c are given in Canuto et al. (1994).

To solve Eqs. (8b–e) we consider the stationary case. The system of equations (8b–e) then becomes a set of algebraic equations that we have solved using methods of symbolic algebra. The result generalizes the pure convective case (Canuto et al. 1994):

$$\begin{aligned} \tau^{-1} \overline{q^2 w} &= A \frac{\partial \overline{q^2}}{\partial z} + B \frac{\partial \overline{w^2}}{\partial z} + C(g\alpha\tau) \frac{\partial \overline{w\theta}}{\partial z} \\ &+ (g\alpha\tau)^2 D \frac{\partial \overline{\theta^2}}{\partial z} + E \frac{\partial}{\partial z} (\overline{u^2} - \overline{v^2}) + F \frac{\partial}{\partial z} \overline{uv} \\ &+ G \frac{\partial}{\partial z} \overline{uw} + H \frac{\partial}{\partial z} \overline{vw} + g\alpha\tau l \frac{\partial}{\partial z} \overline{u\theta} \\ &+ g\alpha\tau J \frac{\partial}{\partial z} \overline{v\theta}. \end{aligned} \quad (9a)$$

Contrary to the DGA (8a), Eq. (9a) entails the gradients of all the second-order moments, $\overline{q^2}$, $\overline{w^2}$, $\overline{w\theta}$, etc., which will be given below, Eqs. (14)–(16). All the “turbulent diffusivities” τA , τB , τC , . . . have the general form

$$DA = A_1 \overline{w^2} + A_2 g\alpha\tau \overline{w\theta} + A_3 \overline{uw} + A_4 \overline{vw}. \quad (9b)$$

The dimensionless coefficient A_i and the denominator D are algebraic functions of the dimensionless variables τN^2 and $\tau^2 \Sigma^2$, where Σ is the mean shear. To facilitate the use, a numerical code is available upon request that gives the functions A , . . . , J of Eq. (9a).

4. The complete model

The procedure is as follows. We insert (7a) and (7c) into Eqs. (2a) and (3a). In its general form, the resulting equations are too complex to be used in an ocean model, and one must reduce their complexity while preserving the main physical features. The methodology that we follow is well founded physically: due to the wide spectrum of eddies, one chooses a variable to represent the large scales (the turbulent kinetic energy) and another variable to represent the small scales that contain little energy but have a large vorticity (the dissipation ϵ). The *resulting model* is the K - ϵ model. To obtain the Reynolds stresses b_{ij} and the heat fluxes h_i , we adopt the ARSM (algebraic Reynolds stress model). In its simplest representation, the model amounts to neglecting the D/D_t and the diffusion terms in Eqs. (2a), (3a), and (4a). The resulting equations become algebraic; specifically, they are a system of coupled linear equations:

Reynolds stresses:

$$\begin{aligned} b_{ij} &= \tau_{ij} - \frac{2}{3} K \delta_{ij} \\ &= -\lambda_1 \tau K S_{ij} + \lambda_4 \tau B_{ij} - \lambda_2 \tau \Sigma_{ij} - \lambda_3 \tau Z_{ij} \end{aligned} \quad (10a)$$

heat flux h_i :

$$A_{ik} h_k = -(K_h)_{ij} \frac{\partial T}{\partial x_j} \quad (10b)$$

The tensors A_{ij} and $(K_h)_{ij}$ are defined by

$$\begin{aligned} A_{ij} &= \lambda_5 \delta_{ij} + \lambda_8 \tau^2 \lambda_i T_{.j} + \lambda_6 \tau S_{ij} + \lambda_7 \tau V_{ij} \\ (K_h)_{ij} &= \tau \left(b_{ij} + \frac{2}{3} \delta_{ij} K \right). \end{aligned} \quad (10c)$$

Furthermore, \mathbf{B} , $\mathbf{\Sigma}$, and \mathbf{Z} are defined as

$$B_{ij} = \lambda_i h_j + \lambda_j h_i - \frac{2}{3} \delta_{ij} \lambda_k h_k \quad (11a)$$

$$\Sigma_{ij} = S_{ik} b_{kj} + S_{jk} b_{ik} - \frac{2}{3} \delta_{ij} S_{kl} b_{kl} \quad (11b)$$

$$Z_{ij} = b_{ik} V_{jk} + b_{jk} V_{ik}, \quad (11c)$$

where shear S_{ij} and vorticity V_{ij} have already been defined. In order to homogenize the notation, we have introduced the dimensionless constants:

$$\begin{aligned} \lambda &= \frac{\tau_{pv}}{\tau}, & \lambda_1 &= \frac{4}{15} \lambda, & \lambda_2 &= \frac{1}{2} (1 - \alpha_1) \lambda, \\ \lambda_3 &= \frac{1}{2} (1 - \alpha_2) \lambda, & \lambda_4 &= \frac{1}{2} \beta_5 \lambda, & \lambda_5 &= \frac{\tau}{\tau_{p\theta}}, \\ \lambda_6 &= 1 - \frac{3}{4} \alpha_3, & \lambda_7 &= 1 - \frac{5}{4} \alpha_3, & \lambda_8 &= (1 - \gamma_1) \frac{\tau_\theta}{\tau}. \end{aligned} \quad (12)$$

Equations (5a–d) for K and ϵ have remained unchanged.

5. Shear and arbitrary stratification

Here, we present the analytic solution of Eqs. (10a–c) for the following case:

$$\frac{\partial T}{\partial x_i} \rightarrow \frac{\partial T}{\partial z} \delta_{i3}, \quad U_i = [U(z), V(z), 0]. \quad (13a)$$

The shear and vorticity acquire the form

$$\begin{aligned} \mathbf{S}_{ij} &= \frac{1}{2} \begin{pmatrix} 0 & 0 & \partial U / \partial z \\ 0 & 0 & \partial V / \partial z \\ \partial U / \partial z & \partial V / \partial z & 0 \end{pmatrix}, \\ \mathbf{V}_{ij} &= \frac{1}{2} \begin{pmatrix} 0 & 0 & \partial U / \partial z \\ 0 & 0 & \partial V / \partial z \\ \partial U / \partial z & -\partial V / \partial z & 0 \end{pmatrix}. \end{aligned} \quad (13b)$$

Eqs. (10a–c) are then solved using methods of symbolic algebra. The results are

Reynolds stresses:

$$\overline{uw} = -K_m \frac{\partial U}{\partial z}, \quad \overline{vw} = -K_m \frac{\partial V}{\partial z} \quad (14a)$$

$$\overline{uv} = (\lambda_2 + \lambda_3) \tau K_m \frac{\partial U}{\partial z} \frac{\partial V}{\partial z} \quad (14b)$$

Timescale:

$$\frac{1}{2} \tau = \frac{K}{\epsilon} \quad (14c)$$

Turbulent kinetic energies:

$$\begin{aligned} \overline{u^2} = & \frac{2}{3}K + \frac{1}{3}\tau K_m \left[(\lambda_2 + 3\lambda_3) \left(\frac{\partial U}{\partial z} \right)^2 - 2\lambda_2 \left(\frac{\partial V}{\partial z} \right)^2 \right] \\ & + \frac{2}{3}\lambda_4 K_h \tau N^2 \end{aligned} \quad (15a)$$

$$\begin{aligned} \overline{v^2} = & \frac{2}{3}K + \frac{1}{3}\tau K_m \left[(\lambda_2 + 3\lambda_3) \left(\frac{\partial U}{\partial z} \right)^2 - 2\lambda_2 \left(\frac{\partial U}{\partial z} \right)^2 \right] \\ & + \frac{2}{3}\lambda_4 K_h \tau N^2 \end{aligned} \quad (15b)$$

$$\overline{w^2} = \frac{2}{3}K + \frac{1}{3}(\lambda_2 - 3\lambda_3)K_m \tau \Sigma^2 - \frac{4}{3}\lambda_4 K_h \tau N^2 \quad (15c)$$

Mean shear, temperature gradient and Richardson number:

$$\begin{aligned} \Sigma^2 \equiv & \left(\frac{\partial U}{\partial z} \right)^2 + \left(\frac{\partial V}{\partial z} \right)^2, \quad N^2 = g\alpha \frac{\partial T}{\partial z}, \\ \text{Ri} \equiv & N^2 \Sigma^{-2} \end{aligned} \quad (15d)$$

Heat fluxes:

$$\overline{w\theta} = -K_h \frac{\partial T}{\partial z} \quad (16a)$$

$$\overline{u\theta} = \lambda_5^{-1} \left[K_m + \frac{1}{2}(\lambda_6 + \lambda_7)K_h \right] \tau \frac{\partial T}{\partial z} \frac{\partial U}{\partial z} \quad (16b)$$

$$\overline{v\theta} = \lambda_5^{-1} \left[K_m + \frac{1}{2}(\lambda_6 + \lambda_7)K_h \right] \tau \frac{\partial T}{\partial z} \frac{\partial V}{\partial z} \quad (16c)$$

Turbulent momentum and heat diffusivities:

$$K_m = 2S_m \frac{K^2}{\epsilon}, \quad K_h = 2S_h \frac{K^2}{\epsilon} \quad (16d)$$

Structure functions $S_{m,h}$:

$$DS_m = s_0 + s_1(\tau N)^2 + s_2(\tau \Sigma)^2 \quad (17a)$$

$$DS_h = s_4 + s_5(\tau N)^2 + s_6(\tau \Sigma)^2 \quad (17b)$$

$$\begin{aligned} D = & d_0 + d_1(\tau N)^2 + d_2(\tau \Sigma)^2 + d_3(\tau N)^4 \\ & + d_4(\tau^2 N \Sigma)^2 + d_5(\tau \Sigma)^4 \end{aligned} \quad (17c)$$

Dimensionless variables s_k :

$$s_0 = \frac{3}{2}\lambda_1 \lambda_5^2 \quad (18a)$$

$$\begin{aligned} s_1 \equiv & -\lambda_4(\lambda_6 + \lambda_7) + 2\lambda_4 \lambda_5 \left(\lambda_1 - \frac{1}{3}\lambda_2 - \lambda_3 \right) \\ & + \frac{3}{2}\lambda_1 \lambda_5 \lambda_8 \end{aligned} \quad (18b)$$

$$s_2 \equiv -\frac{3}{8}\lambda_1(\lambda_6^2 - \lambda_7^2), \quad s_4 \equiv 2\lambda_5, \quad (18c)$$

$$s_5 = 2\lambda_4 \quad (18c)$$

$$\begin{aligned} s_6 = & \frac{2}{3}\lambda_5(3\lambda_3^2 - \lambda_2^2) - \frac{1}{2}\lambda_5 \lambda_1(3\lambda_3 - \lambda_2) \\ & + \frac{3}{4}\lambda_1(\lambda_6 - \lambda_7) \end{aligned} \quad (18d)$$

Dimensionless variables d_k :

$$d_0 = 3\lambda_5^2 \quad (19a)$$

$$d_1 \equiv \lambda_5(7\lambda_4 + 3\lambda_8), \quad (19b)$$

$$d_2 \equiv \lambda_5^2(3\lambda_3^2 - \lambda_2^2) - \frac{3}{4}(\lambda_6^2 - \lambda_7^2) \quad (19b)$$

$$d_3 \equiv \lambda_4(4\lambda_4 + 3\lambda_8), \quad (19c)$$

$$d_5 \equiv \frac{1}{4}(\lambda_2^2 - 3\lambda_3^2)(\lambda_6^2 - \lambda_7^2) \quad (19c)$$

$$\begin{aligned} d_4 \equiv & \lambda_4[\lambda_2 \lambda_6 - 3\lambda_3 \lambda_7 - \lambda_5(\lambda_2^2 - \lambda_3^2)] \\ & + \lambda_5 \lambda_8(3\lambda_3^2 - \lambda_2^2). \end{aligned} \quad (19d)$$

Some general considerations are in order. As expected, the structure functions $S_{m,h}$ depend on the two independent variables that represent the external fields of stratification N and shear Σ , as well as on the turbulent timescale τ . As one can notice, N and Σ enter in a symmetric manner in $S_{m,h}$, that is, the exponents are symmetric. This is not the case with the MY-type models, for they lack the terms s_2 and d_5 , which are solely due to the new term in the pressure correlation (7c), specifically, the coefficient α_3 , which is zero in these models. That makes $\lambda_6 = \lambda_7 = 1$ [see Eq. (12)], and thus $s_2 = 0$, $d_5 = 0$; see Eqs. (18c,d). In these models, the maximum powers of Σ and N are 2 and 4. See, for example, Eqs. (20)–(21) of Hassid and Galperin (1983) in which, in addition, the numerator of S_m does not depend on shear, while that of S_h does, a somewhat counterintuitive result.

6. Model constants

The model constants are determined using two methodologies that yield very similar results. The first approach uses a previous theoretical turbulence model based in part on RNG (Renormalization Group) methods and whose predictions were tested on different types of turbulent flows (Canuto and Dubovikov 1996a,b, 1997a,b). Since the model contains no adjustable parameters, the predictions are unique:

$$\begin{aligned} \tau_{pv} \tau^{-1} = & \frac{2}{5}, \quad \tau \tau_{p\theta}^{-1} = 5(1 + \sigma_r^{-1}), \\ \tau_\theta \tau^{-1} = & \sigma_r, \quad \sigma_r = 0.72, \quad \gamma_1 = \frac{1}{3}, \\ \beta_5 = & \frac{1}{2}. \end{aligned} \quad (20a)$$

The values of the λ defined in Eq. (12) are then as follows: Model A:

$$\begin{aligned} &(\lambda_1, \lambda_2, \lambda_3, \lambda_4, \lambda_5, \lambda_6, \lambda_7, \lambda_8) \\ &= (0.107, 0.0032, 0.0864, 0.12, 11.9, 0.4, 0, 0.48) \end{aligned} \quad (20b)$$

Model B: We begin by adopting the expressions (Shih and Shabbir 1992; Canuto 1994):

$$\begin{aligned} \lambda_2 &= (1 - \alpha_1)(2c_4^*)^{-1}, & \lambda_3 &= (1 - \alpha_2)(2c_4^*)^{-1}, \\ \lambda_4 &= \beta_5(2c_4^*)^{-1}, & \lambda_6 &= 1 - \frac{3}{4}\alpha_3, \\ \lambda_7 &= 1 - \frac{5}{4}\alpha_3, & \lambda_8 &= (1 - \gamma_1)\frac{\tau_\theta}{\tau}, \end{aligned} \quad (21a)$$

where

$$\begin{aligned} c_4^* &= 2 + 6.22F^2(1 - F)^{3/4} - F^{1/2}, & \alpha_1 &= 6\alpha_5, \\ \alpha_2 &= \frac{2}{3}(2 - 7\alpha_5), & \alpha_3 &= \frac{4}{5}, \\ \alpha_5 &= \frac{1}{10}\left(1 + \frac{4}{5}F^{1/2}\right), & F &= 0.64, & \beta_5 &= 0.48. \end{aligned} \quad (21b)$$

The λ thus obtained are

$$\begin{aligned} &(\lambda_2, \lambda_3, \lambda_4, \lambda_6, \lambda_7) \\ &= (0.00336, 0.0906, 0.101, 0.4, 0). \end{aligned} \quad (21c)$$

To determine $\lambda_{1,5}$, we employ a neutral surface layer in which the mean profiles are logarithmic, the mean wind is along the x direction, and z approaches zero. Thus,

$$-\overline{uw} = u_*^2, \quad \tau \frac{dU}{dz} = \left(\frac{q}{u_*}\right)^2, \quad \frac{1}{2}q^2 \equiv K. \quad (21d)$$

Under these conditions, the algebraic equations for $\overline{u^2}$, $\overline{v^2}$, and $\overline{w^2}$, Eqs. (15a-c), yield

$$\lambda_1 = \frac{4}{3}(3\lambda_3^2 - \lambda_2^2) + 4B_1^{-4/3}, \quad (21e)$$

where $B_1 \equiv (q/u_*)^3 = 16.6$ in accord with the MY model. Using $\lambda_{2,3}$ from (20b), we obtain

$$\lambda_1 = 0.127. \quad (21f)$$

The value of λ_5 is obtained in a similar fashion. Assuming that production equals dissipation in the above neutral surface layer, we have

$$S_h = 2B_1^{-4/3}\sigma_{i_0}^{-1}, \quad \sigma_{i_0} = 1, \quad (21g)$$

where σ_{i_0} is the turbulent Prandtl number in the neutral case, which we take to be unity. Applying the neutral condition and $z \rightarrow 0$ to the equations for $u\theta$, $w\theta$ [Eqs. (16b,c)] and using

$$\overline{w\theta} = -K\tau S_h \frac{dT}{dz}, \quad (21h)$$

after some algebra we obtain an algebraic equation for λ_5 :

$$\begin{aligned} \lambda_5^2 - \frac{1}{3}B_1^{4/3}(1 + \lambda_2 - 3\lambda_3)\sigma_{i_0}\lambda_5 \\ - \frac{1}{4}(\lambda_6 - \lambda_7)B_1^{4/3}(\lambda_6 + \lambda_7 + 2\sigma_{i_0}) = 0. \end{aligned} \quad (21i)$$

The solution is

$$\lambda_5 = 11.2. \quad (21j)$$

Similarly, from the algebraic equation for $\overline{\theta^2}$, we have

$$\frac{\tau_\theta}{\tau} = \sigma_{i_0}^{-1}B_1^{-2/3}Q, \quad Q \equiv \overline{\theta^2}u_*^2/(\overline{w\theta})_s^2 = 3.1, \quad (22a)$$

where the subscript s indicates a surface quantity, and $Q = 3.1$ in accordance with Mellor and Yamada (1982). Substituting (22a) into (21a) and using $\gamma_1 = 1/3$ gives

$$\lambda_8 = (1 - \gamma_1)\frac{\tau_\theta}{\tau} = 0.318. \quad (22b)$$

Thus, finally,

$$\begin{aligned} &(\lambda_1, \lambda_2, \lambda_3, \lambda_4, \lambda_5, \lambda_6, \lambda_7, \lambda_8) \\ &= (0.127, 0.00336, 0.0906, 0.101, 11.2, 0.4, \\ &0, 0.318). \end{aligned} \quad (22c)$$

As one can observe, the two approaches yield very similar results.

7. Critical Ri

There is more than one definition of a critical Ri, depending on the specific physical feature that one aims to describe, and this has created some confusion as to which one is applicable in practical cases. From the theoretical viewpoint, Miles (1961) and Howard (1961) used linear stability analysis and established that for linear stability to exist the necessary, but not sufficient, condition is

$$\text{Ri} > 1/4. \quad (23)$$

This result has been interpreted to mean that turbulence cannot exist for $\text{Ri} > 1/4$, even though this is hardly a justifiable inference since by construction (23) says nothing about nonlinearities and thus turbulence. And yet, most models of either atmospheric and/or oceanic turbulent mixing assume (23). Nonlinear interactions were included by Abarbanel et al. (1984), who derived the *sufficient* and *necessary* condition for stability to be

$$\text{Ri} > 1. \quad (24)$$

The first approach leading to (23) can be called ‘‘bottom-up’’ (from linear stability), while the second ap-

proach leading to (24) is “top-down,” since it starts from the full nonlinear interactions and inquires when such nonlinearities, and thus turbulence, cease to exist. Since, in dealing with atmospheric and oceanic mixing problems, one can hardly follow the setting in of the linear instabilities that ultimately lead to turbulence, it seems that from an operational viewpoint (24) is the relevant condition since it tells us when turbulence can no longer be sustained against the effect of stable stratification. And yet, (23) has been widely used instead of (24). However, a variety of data favor (24) not (23): (i) The first empirical evidence was presented in the study by Martin (1985), who showed that in order to obtain the correct mixed layer depths at OWS Papa and November he had to let turbulent mixing occur up to $Ri \sim 1$; (ii) Even before Martin’s study, evidence was available that turbulence existed at least up to $Ri \sim 1$; early laboratory data by Taylor (cited in Monin and Yaglom 1971) showed that turbulent exchange exists even when $Ri > 1$, and in 1964 Webster’s laboratory measurements of turbulence in stably stratified flows (see Fig. 3) showed that mixing persists up to $Ri \sim 1$; (iii) More recently, LES (large eddy simulations: Wang et al. 1996; see Fig. 7) and DNS (direct numerical simulations: Gerz et al. 1989) also showed that turbulence exists up to $Ri \sim 1$.

The question then arises: do turbulence models yield (23) or (24)? The way to the answer is as follows. Using Eqs. (14a), (15d), and (16a) we have

$$P_s = -\tau_{ij}S_{ij} = K_m \Sigma^2, \quad P_b = g\alpha w\bar{\theta} = -K_h N^2, \quad (25a)$$

and thus the equilibrium condition $P = P_s + P_b = \epsilon$ becomes

$$\epsilon = K_m \Sigma^2 - K_h N^2 = 2 \frac{K^2}{\epsilon} (S_m \Sigma^2 - S_h N^2). \quad (25b)$$

Using $\tau = 2K\epsilon^{-1}$, the dimensionless variable $y \equiv (\tau \Sigma)^2$, and the $S_{m,h}$ given by Eqs. (17a–c) a little algebra transforms (25b) into a relation for $y(Ri)$:

$$A(Ri)y^2 + B(Ri)y + C = 0, \quad (26a)$$

where the functions A and B are given by

$$A(Ri) \equiv (s_5 + 2d_3)Ri^2 - (s_1 - s_6 - 2d_4)Ri - s_2 + 2d_5 \quad (26b)$$

$$B(Ri) = (s_4 + 2d_1)Ri - s_0 + 2d_2, \quad (26c)$$

Since we are using a turbulence model and not linear stability analysis, the only approach is the top-down: Ri_{cr} is defined as the value of Ri above which turbulent mixing ceases to exist (due to the effect of stable stratification). Since the mixing coefficient (diffusivity) is proportional to the eddy velocity $w \sim K^{1/2}$, in the limit $K \rightarrow 0$ we have $y \rightarrow \infty$, and Eq. (26a) can be satisfied only if $A(Ri_{cr}) = 0$. Using (26b), this becomes the equation for Ri_{cr} :

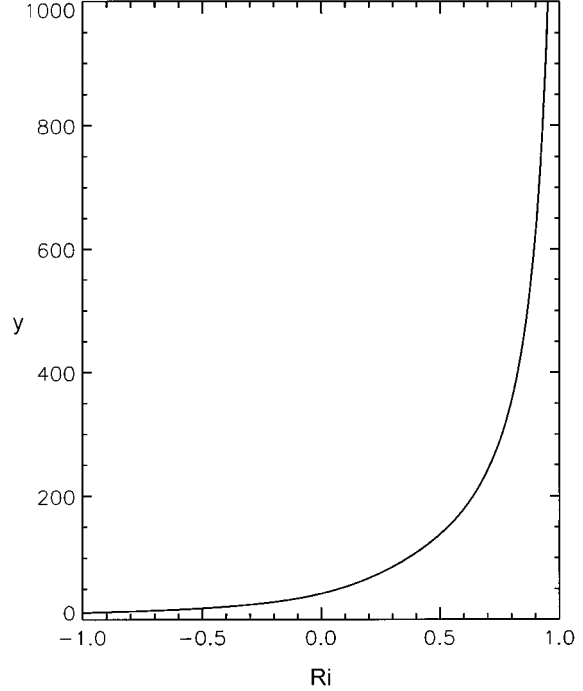


FIG. 1. The timescale τ , specifically the variable y vs the degree of stability Ri . Since y is the inverse of the turbulent kinetic energy K , the figure shows that at $Ri_{cr} \sim 1$, K vanishes because the stratification becomes too strong for turbulent mixing to survive. The MY-type models predict a far smaller $Ri_{cr} \sim 0.20$, which considerably reduces the extent of turbulent mixing.

$$Ri_c = (2c_1)^{-1}[-c_2 + (c_2^2 - 4c_1c_3)^{1/2}], \quad (26d)$$

where the constants are

$$c_1 \equiv s_5 + 2d_3, \quad c_2 \equiv -s_1 + s_6 + 2d_4, \quad (26e)$$

$$c_3 \equiv -s_2 + 2d_5.$$

Using the constants discussed in section 6, we obtain two values:

$$Ri_c = 0.85 \quad \text{and} \quad Ri_c = 1.03, \quad (27a)$$

which are indeed of the form (24). Thus, the inclusion of the full pressure correlations has brought the turbulence model to agree with the general result of Abarbanel et al. (1984). To make the case complete, we notice that, as discussed earlier, the MY-type models have $s_2 = d_5 = 0$ in which case (26b) gives

$$Ri_{cr}(MY) = (s_1 - s_6 - 2d_4)(s_5 + 2d_3)^{-1} = 0.195, \quad (27b)$$

which is of the form (23).

The function $y(Ri)$ is plotted in Fig. 1. As one reaches a value of $Ri_{cr} \sim 1$, the function y tends to infinity. The two structure functions $S_{m,h}$ versus Ri are plotted in Fig. 2 [the equivalent MY (1984) curves are plotted in their Fig. 4]. The left-hand side of the figure is for unstable stratification ($Ri < 0$), while the right-hand side is for stable stratification ($Ri > 0$). As one can expect, the

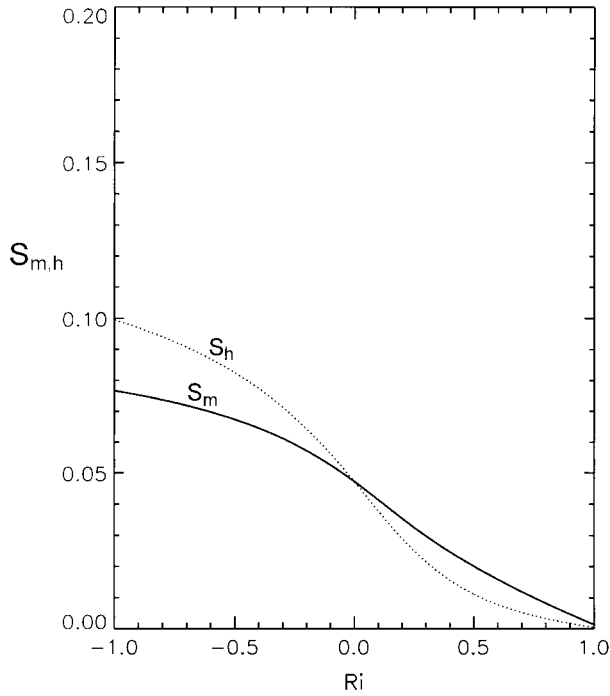


FIG. 2. Model predictions for the dimensionless structure functions S_m and S_h defined in Eq. (22a) vs the degree of stability Ri . The $P = \epsilon$ condition is used.

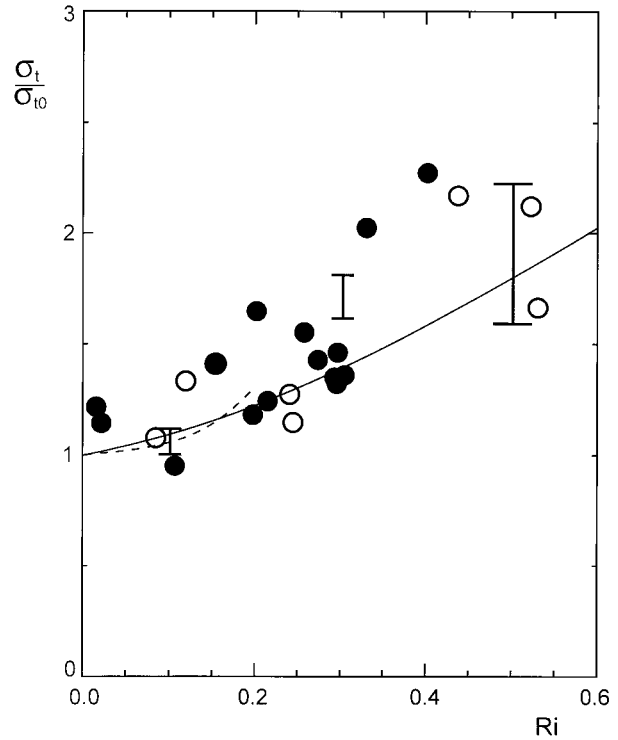


FIG. 3. Laboratory and numerical simulation data for the turbulent Prandtl number σ_T vs Ri (Webster 1964; Gerz et al. 1989); σ_T is defined in Eq. (29a). The short dashed line corresponds to the MY-type models that are valid only for $Ri_{cr} \leq 0.2$.

relative position of the curves switches as one moves from negative to positive Ri . In the unstable case, the heat diffusivity is larger than the momentum diffusivity since one expects that the temperature gradient affects more the heat diffusivity than the momentum diffusivity.

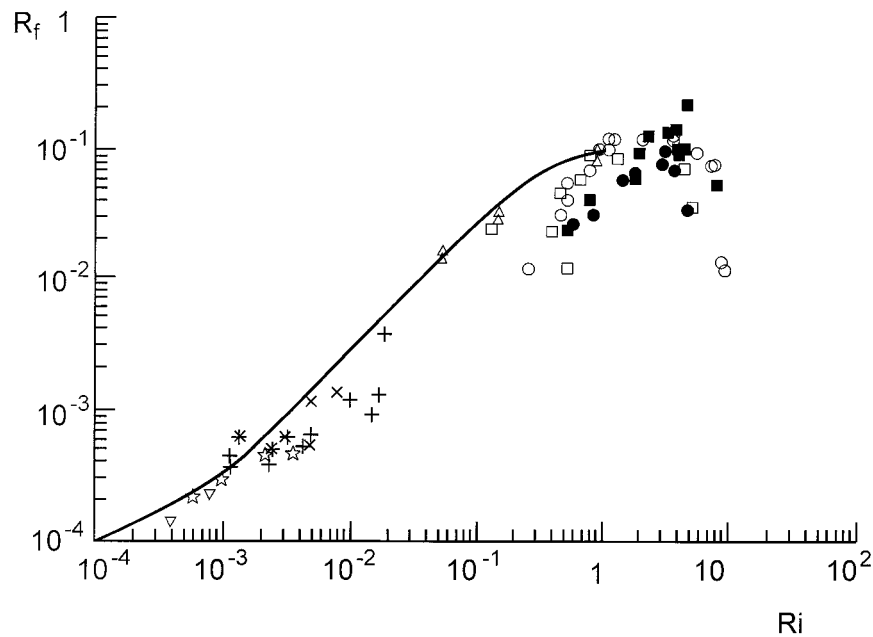


FIG. 4. The turbulent flux Richardson number R_f vs Ri , Eq. (29b). The symbols refer to the different authors cited in Maderich et al. (1995) and correspond to either grid-generated turbulence and/or to freely decaying turbulence in a stably stratified medium.

The reverse is true when stratification is stable. The lower value of S_h versus S_m is in accord with the laboratory data for the turbulent Prandtl number, which we discuss below in section 8d. A comment may be useful concerning Fig. 1 of Galperin et al. (1988), where $S_{m,h}$ are plotted not versus Ri but versus $(\tau N)^2$. Even though we could do the same with the present model, we find such representation less transparent than the one versus Ri because it still uses the turbulent variable τ , which has not been explicitly solved for and which is a function of Ri. In fact, one has

$$(\tau N)^2 = y(\text{Ri})\text{Ri}, \quad (27c)$$

and since Eqs. (26a–c) give $y(\text{Ri})$, we have found it more transparent to plot $S_{m,h}$ versus the external fields (N and Σ) rather than to use the mixed representation $(\tau N)^2$.

8. Tests of the model

a. Mixed layer studies

Burchard and Bolding (2001) have recently used the above K – ϵ model to study the ocean mixed layer (ML) and compared the results with those of previous models. In this paper, we shall therefore apply the new turbulence model only to the global ocean, together with a new model for the diffusivities below the mixed layer discussed in section 9. We deem it important, however, to first present a set of tests not directly related to oceanography, but that are important to assess the reliability of the model.

b. Unstable stratification, $\text{Ri} \rightarrow \infty$

A relevant test concerns the case of thermal convection (no shear and unstable stratification, $N^2 < 0$) for which an ample set of both numerical and laboratory data are available (Canuto and Dubovikov 1997a). The widely used mixing length theory yields

$$\overline{w\theta} = K_h \left| \frac{\partial T}{\partial z} \right| \sim (g\alpha)^{1/2} \Lambda^2 \left| \frac{\partial T}{\partial z} \right|^{3/2}, \quad (28a)$$

where Λ is the mixing length. The question is whether the previous turbulence model can reproduce (28a). We shall only sketch the steps necessary. With no shear, Eq. (25b) becomes $\tau^2 |N^2| S_h = 2$. Substituting the corresponding expression for S_h from (17b,c),

$$S_h = 2[3\lambda_5 - (4\lambda_4 + 3\lambda_8)\tau^2 |N^2|]^{-1}. \quad (28b)$$

The results are

$$\tau^2 |N^2| = \text{const}, \quad S_h = \text{const}. \quad (28c)$$

Since $g\alpha J = \epsilon$, with $J \equiv \overline{w\theta}$, we have from Eqs. (16a,d)

$$J \sim (g\alpha)^{-1} KN. \quad (28d)$$

Using the Kolmogorov law $K = (\epsilon k_0^{-1})^{2/3}$, we eliminate K and obtain ($k_0 \sim \Lambda^{-1}$):

$$J \sim (g\alpha)^{-1} \Lambda^2 N^3 \sim (g\alpha)^{1/2} \Lambda^2 \left| \frac{\partial T}{\partial z} \right|^{3/2}, \quad (28e)$$

which coincides with (28a).

c. Pure shear case, $\text{Ri} \rightarrow 0$

Since this is a case of interest to engineering flows, it has been widely studied (Rodi 1976). To first order in the shear, we have from Eqs. (17a,c) that

$$S_m = \frac{S_0}{d_0}, \quad S_m = \frac{4}{75}. \quad (28f)$$

Thus, the first of (16d) becomes

$$K_m = C_\mu \frac{K^2}{\epsilon}, \quad C_\mu = 0.11, \quad (28g)$$

which is a well-known formula employed in shear flows studies (Rodi 1976).

d. Turbulent Prandtl number versus Ri relation

Data on the relationship,

$$\sigma_t(\text{Ri}) \equiv \frac{K_m}{K_h} \text{ versus Ri}, \quad (29a)$$

have been available for a long time (Webster 1964). More recently, Gerz et al. (1989) have carried out a direct numerical simulation of stratified turbulent shear flow and added new data. In Fig. 3 we have collected these data and superimposed on them the model results corresponding to the equilibrium case. The model results reproduce the data quite well.

e. Flux Richardson number versus Ri relation

A set of data is available (Maderich et al. 1995) that provides the flux Richardson number versus Ri relationship, where

$$R_f \equiv \text{Ri} \sigma_t^{-1}(\text{Ri}). \quad (29b)$$

Using the equilibrium solution, the model results are exhibited in Fig. 4.

f. The representation $K_h = \Gamma \epsilon N^{-2}$

Several authors (Thorpe 1977; Osborne 1980; Oakey 1982; Moum 1989; Davis 1994; Toole et al. 1994; Wuest et al. 1996) have represented K_h as

$$K_h = \Gamma \frac{\epsilon}{N^2}, \quad \Gamma = R_f(1 - R_f)^{-1}. \quad (29c)$$

The “measured” values of Γ are

$$0.12 \leq \Gamma \leq 0.48. \quad (29d)$$

The function $\Gamma(\text{Ri})$ versus Ri is exhibited in Fig. 5: a value $\Gamma = 1/4$ at $\text{Ri} = 1/4$ (e.g., Oakey 1982; Toole et al. 1994) is reproduced by the model. A word of caution

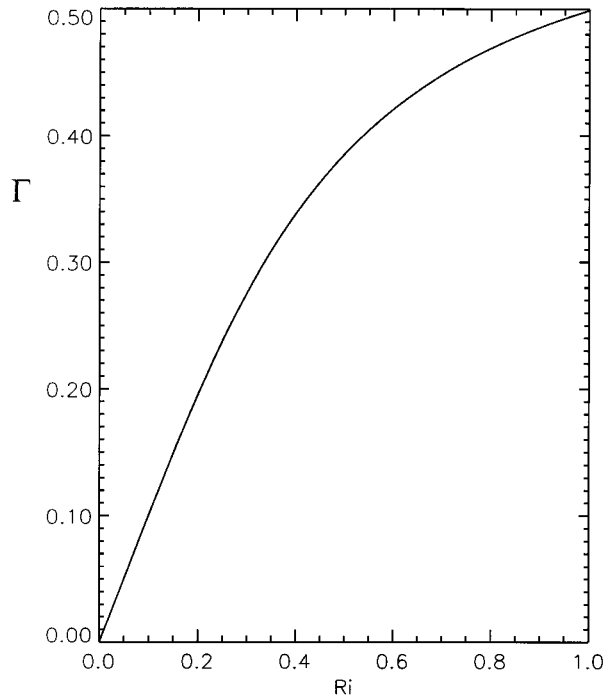


FIG. 5. Efficiency parameter $\Gamma(\text{Ri})$, Eq. (29c) vs Ri . The predicted value $\Gamma \sim 1/4$, at $\text{Ri} \sim 1/4$ is well within the measured estimates [see references after Eq. (29d)].

is required, however. Care must be exercised since in general the heat diffusivity K_h is not the same as the “mass diffusivity” K_ρ defined via the relation

$$\overline{\rho'w''} = -K_\rho \frac{\partial \rho}{\partial z}. \quad (29e)$$

In fact, it is easy to derive the relation

$$K_\rho = K_h \left(1 - \frac{K_s}{K_h} R_\rho \right) (1 - R_\rho)^{-1},$$

$$R_\rho = \frac{\alpha_s \partial S / \partial z}{\alpha \partial T / \partial z}, \quad (29f)$$

where K_s is the salt diffusivity and R_ρ is the Turner number (α_s is the haline contraction coefficient). As in the present case, $K_s = K_h$; it follows that $K_h = K_\rho$.

9. New model for mixing below the mixed layer

All global ocean models require that one prescribe the mixing below the mixed layer. Since we do not have a detailed model for the internal wave breaking phenomena that are thought to generate the mixing, the diffusivities for momentum, heat, and salinity below the ML have been traditionally assumed to be adjustable parameters (background diffusivities). For example, the National Center for Atmospheric Research model, to be discussed below, uses the following values:

$$K_m = 16.7 \text{ cm}^2 \text{ s}^{-1}, \quad K_h = K_s = 0.5 \text{ cm}^2 \text{ s}^{-1}. \quad (30a)$$

It would be preferable not to use (30a) and to try to model $K_{m,h}$. In this paper, we avoid (30a), suggest an alternative procedure, and use it in the global ocean model. Our main assumption is that the turbulence model described in the previous sections has given us the correct functional dependence of the $K_{m,h}$ on Ri and, if so, the diffusivities ought to be formally valid below the ML as well. The key problem is to *define and compute* Ri below the mixed layer. We suggest using the measured data of the vertical shear generated by the wave breaking phenomenon (Gargett et al. 1981). By integrating over all wavenumbers, one can compute the shear due to internal waves, which we denote Σ_{wb} (for wave breaking) to distinguish it from Σ , which was used above to denote the wind shear. One can then form a corresponding Ri_{wb} as follows:

$$\text{Ri}_{\text{wb}} = N^2 / \Sigma_{\text{wb}}^2. \quad (30b)$$

Early arguments by Munk (1966) suggesting that $\text{Ri}_{\text{wb}} \sim 1$ were confirmed by Gargett et al. (1981, sec. 5). To those arguments, we add the following consideration. As the value of Ri_{cr} above, for which there is no longer turbulent mixing as computed from our model, is $O(1)$; if $\text{Ri}_{\text{wb}} \gg 1$, there would be no turbulence generated by the internal waves at all. On the other hand, if $\text{Ri}_{\text{wb}} \ll 1$, there would be very strong turbulence producing a viscosity sufficient to damp out the waves themselves. The wave-generated turbulence is thus self-limiting. Since the turbulence model gives a precise value for Ri_{cr} while the above argument only tells us that $\text{Ri}_{\text{wb}} \sim O(1)$, we write:

$$\text{Ri}_{\text{wb}} = c \text{Ri}_{\text{cr}}, \quad (30c)$$

where c is a constant reasonably close to unity. We have found that $c = 0.88$ gives a diffusivity close to that measured by Ledwell et al. (1993).

10. Global Ocean GCM

To test the new vertical diffusivities, we used the NCAR Climate System Model Ocean Model (NCAR Oceanography section 1996). We employed the stand-alone $3^\circ \times 3^\circ$ configuration of the model detailed in their technical note with the default parameter values. It has 3.6° spacing in longitude and a variable spacing in latitude increasing from 1.8° at the equator to 3.4° at 17°N , S and then decreasing back to 1.8° for 60°N , S and poleward. There are 25 levels of increasing thickness in the vertical, with the surface level 6 m thick. The option for the Gent–McWilliams (1990) mesoscale eddy parameterization was enabled. Bulk forcing with a seasonal cycle plus a 2-yr timescale restoring condition on the salinity is used, except under sea ice where there is strong (6-day timescale) restoring of both temperature and salinity to climatology. The configuration

and forcing are the same as in Large et al. (1997) for their case B-K. It should be noted, however, that for determination of the length scale in our turbulence model we used the program's definition for mixed layer depth (a buoyancy difference from the surface of $3 \times 10^{-4} \text{ ms}^{-2}$), which is different from that graphed as a diagnostic in Fig. 5 of Large et al. (1997). We initialized our runs with annually averaged Levitus et al. data (Levitus and Boyer 1994; Levitus et al. 1994) and ran for 126 momentum years. As in Large et al. (1994), a 3504-s time step for momentum is used, while for the first 96 momentum years the tracers are accelerated by a factor increasing from 10 at the surface to 100 for the deep ocean. We then set all times steps equal for the remaining 30 years as they did.

11. Results with a local model

In general, the full model is given by Eqs. (5a,d) plus Eqs. (14)–(19). When one deals with a 1D model [e.g., in mixed layer studies, Burchard and Bolding (2001)], one can treat K and ϵ as solutions of the two dynamic equations (5a,d). On the other hand, when dealing with a global ocean model, one must further simplify the problem by reducing the K and ϵ equations to algebraic relations. For K , one uses the local limit of Eq. (5a), which implies that production equals dissipation. Equation (5a) becomes Eq. (25b).

As for the equation for ϵ , the situation is more complex. First, in the local limit $D_f(\epsilon) \rightarrow \Lambda_0^{-1} \epsilon w = \Lambda_0^{-1} \epsilon K^{1/2}$. If one further uses a diffusion–dissipation model, one equates the left-hand side of (5d) to the dissipation term $c_2 \epsilon^2 K^{-1}$. The result is the familiar Kolmogorov law $\epsilon = K^{3/2} \Lambda_0^{-1}$, which requires that we describe Λ_0 somehow. If one keeps the effect of stratification, the same procedure leads to

$$\epsilon = K^{3/2} \Lambda^{-1}, \quad \Lambda = \Lambda_0 (1 + \Lambda_0 |N| K^{-1/2})^{-1}, \quad (31a)$$

which shows that stable stratification suppresses the dissipation length scale. In the “strong stratification” case we further have

$$\Lambda = |N|^{-1} K^{1/2}, \quad (31b)$$

which is Deardorff's (1980) original expression. Equation (31a) then becomes

$$\epsilon = K |N|, \quad (31c)$$

a well-known relation in oceanography (Gargett and Osborn 1981; Gargett 1989). These empirical relations were recently obtained as a particular case of a turbulence model (Cheng and Canuto 1994; Canuto and Cheng 1997), which succeeded in explaining the behavior of Λ found in LES by Schumann (1991). The result was expressed as

$$\Lambda = \Lambda_0 f(N, S), \quad (31d)$$

and the function $f(N, S)$ was given in analytical form. Here we shall use a compromise expression for Λ that

encompasses empirically the effect of stratification and which is easy to use. It is the Deardorff–Blackadar formula:

$$\Lambda = 2^{-3/2} B_1 l, \quad B_1 = 16.6 \quad (32a)$$

$$l = \min\left(\frac{1}{2} \frac{q}{N}, l_1\right) \quad (32b)$$

$$l_1 = \kappa z l_0 (l_0 + \kappa z)^{-1}, \quad l_0 = 0.17H, \quad (32c)$$

where $\frac{1}{2} q^2 = K$ is the turbulent kinetic energy, N is the Brunt–Väisälä frequency, $\kappa = 0.4$ is the von Kármán constant, and H is the mixed layer depth. When used within the NCAR CSM Ocean Model, H is determined as the depth where the buoyancy difference

$$g[\rho(H) - \rho(\text{surface})]\rho(H)^{-1} = 3 \times 10^{-4} \text{ m s}^{-2}. \quad (32d)$$

As for the stratification N , one must use the total density gradient including both salinity and temperature contributions,

$$N^2 = -g\rho^{-1} \frac{\partial \rho}{\partial z} = g \left(\alpha \frac{\partial T}{\partial z} - \alpha_s \frac{\partial S}{\partial z} \right), \quad (32e)$$

where α_s is the haline contraction coefficient. In this paper, we have taken $K_s = K_h$. For the background, we use the same formalism but we replaced l_0 in Eq. (32c) with

$$l_0(\text{wb}) = a k_0^{-1}, \quad a = (3\text{Ko})^{3/2} B_1^{-1}. \quad (33)$$

Here, $\text{Ko} = 1.6\text{--}1.8$ is the Kolmogorov constant. The wavenumber k_0 is the value for the break in slope of the observed spectrum of internal waves (Gargett et al. 1981):

$$k_0 = \frac{1}{10} 2\pi \text{ rad m}^{-1}. \quad (34)$$

Finally, we take the total diffusivities to be

$$K_{m,h} = K_{m,h}(\text{Ri}) + K_{m,h}(\text{Ri}_{\text{wb}}). \quad (35)$$

In the statically unstable case ($\text{Ri} < 0$), we set $K_{m,h}(\text{Ri}_{\text{wb}}) = 0$. The very large mixing due to convective instability makes the background irrelevant in this situation in any case. In adding the diffusivities, we ensured continuity in the transition between regions where external shear dominates and those where the internal wave shear does.

First, we ran the NCAR program as is, with the KPP model (Large et al. 1994), producing the KPP data presented in the figures below. Then, in place of the KPP module, we inserted a module that uses our new model for the diffusivities for momentum and heat, with the salt diffusivity set equal to that of heat. The results are presented in Figs. 6–9 where we exhibit the model results (squares), Levitus data (dashes), and the results using the KPP model (diamonds). We present both the global T and S , as well as for the Atlantic. In Fig. 10 we present the diffusivity profiles at the Canary Islands and in Fig. 11 the northward heat transport.

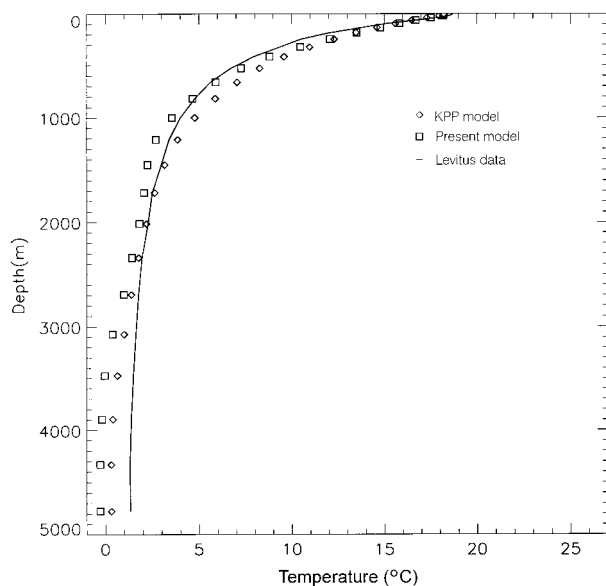


FIG. 6. The resulting global ocean temperature using the OGCM discussed in section 10, with the new model for the background diffusivities discussed in section 9. The Levitus et al. (1994) data are the solid line. We have also run the OGCM code with the KPP model ($K_s = K_h$), and the results are indicated by diamonds. Our model results are shown by squares.

12. Future work and conclusions

The goal of this paper was to construct a model for the vertical diffusivities that contained physical improvements with respect to previous models. The main features of the model can be summarized as follows.

- 1) The model was not tailored to ocean turbulence, as were previous models (e.g., KPP).

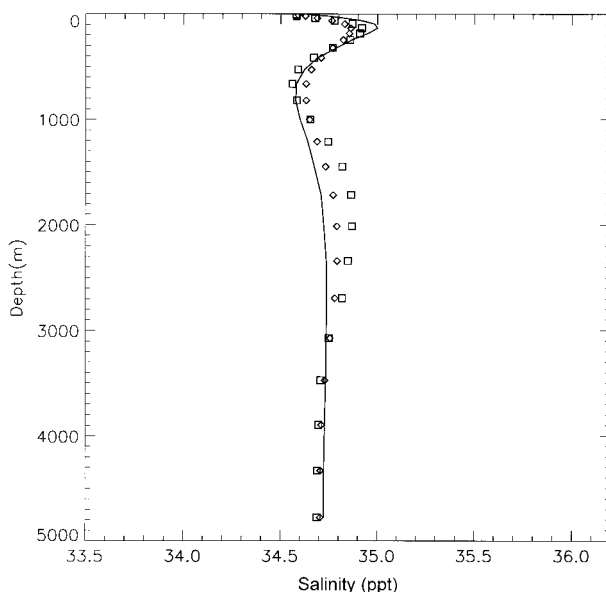


FIG. 7. Same as Fig. 6, but for the global salinity.

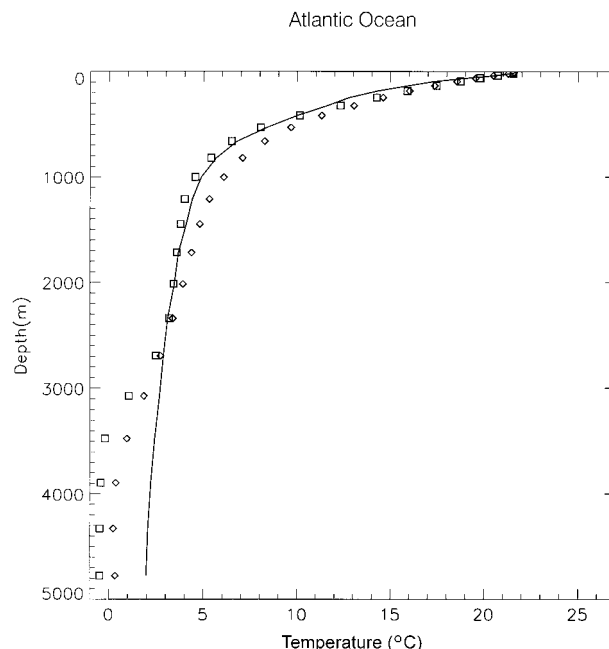


FIG. 8. Same as Fig. 6, but for the Atlantic Ocean.

- 2) The model incorporates advances in turbulent closure modeling. As a by-product, it naturally yields a critical Richardson number of order unity in agreement with mixed layer studies (Martin 1985), laboratory data (Webster 1964; Monin and Yaglom 1971), DNS (Gerz et al. 1989), LES (Wang et al. 1996), and stability analysis that include the nonlinear interactions (Abarbanel et al. 1984).

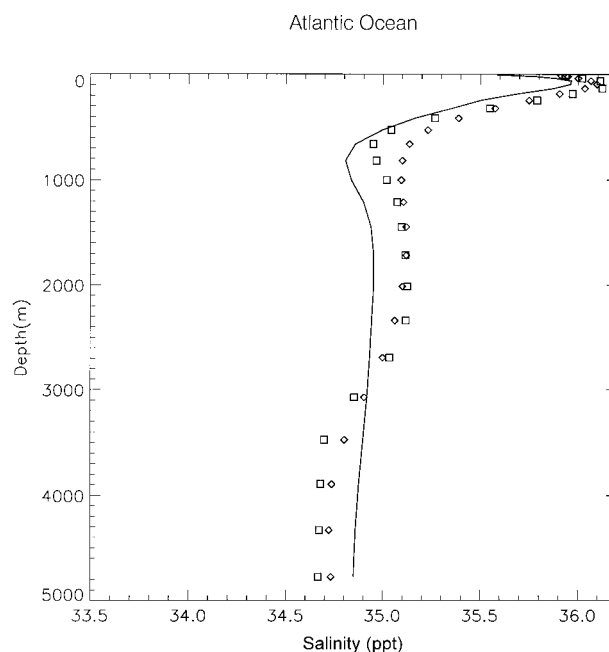


FIG. 9. Same as Fig. 7, but for the Atlantic Ocean.

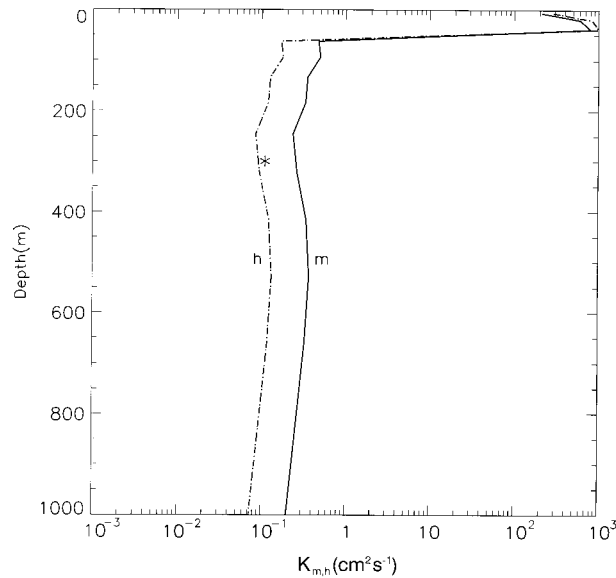


FIG. 10. The diffusivities $K_{m,h}$ ($\text{cm}^2 \text{s}^{-1}$) for North Atlantic Tracer Release Experiment (NATRE). Ledwell et al. (1993) have measured a value of $0.11 \pm 0.02 \text{ cm}^2 \text{s}^{-1}$ at $z = 300 \text{ m}$ (indicated by an asterisk).

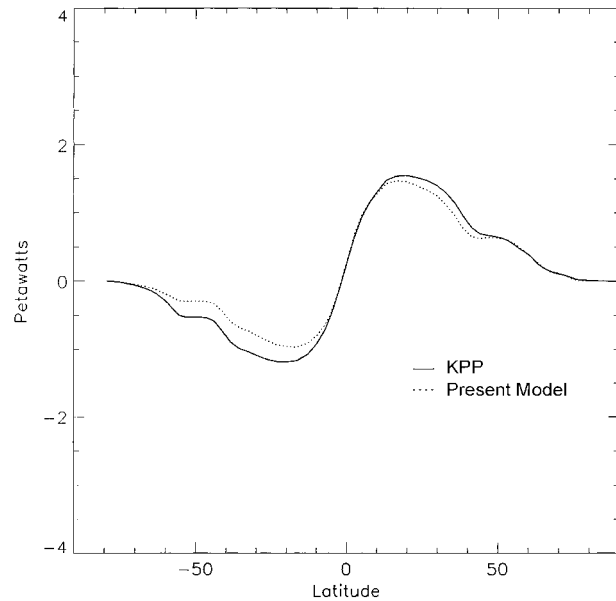


FIG. 11. Polar heat transport vs latitude for the KPP and present model (squares).

- 3) Before using it in an OGCM, the model was shown to reproduce well-documented laboratory, atmospheric, and LES data on stratified turbulence.
- 4) The model reproduces the $K_h = \gamma \epsilon N^{-2}$ representation of the heat diffusivity that has been widely used in the past and predicts a value for γ that varies with Ri , as indeed expected.
- 5) After these tests have been passed, the model is used in an OGCM without altering any of the ingredients that have been used to reproduce the above data.
- 6) One of the strengths of the model is its ability to encompass other cases within the same methodology. Here, we have exploited only the local model, $P = \epsilon$, while it would be very interesting to exploit the new TOM given by Eq. (9a) with a $K-\epsilon$ model, especially in mixed layer studies. Since the new TOM contains considerably more information and is considerably more physical than any previous expression, the effects on ocean mixing should be equally manifest.
- 7) The case of rotation should also be studied more in detail and its effect on the ML and on deep ocean convection investigated. The problem will be taken up in a subsequent paper.
- 8) In the next paper, the model will be extended to include the salinity field, thus allowing K_s to be different than K_h , as dictated by laboratory and ocean data.

Acknowledgments. One of the authors (AH) would like to thank Dr. X. Jiang, Dr. R. Miller, Dr. Z. Garrafo, and J. Johns for invaluable assistance; Dr. G. Danabasoglu for advise with the ocean code, and Dr. T. Rosati and Dr. P. Gent for their hospitality at GFDL and NCAR.

REFERENCES

- Abarbanel, H. D., D. D. Holm, J. E. Marsden, and T. Ratiu, 1984: Richardson number criterion for the non-linear stability of 3D stratified flow. *Phys. Rev. Lett.*, **52**, 2352–2355.
- Baum, E., and E. A. Caponi, 1992: Modeling the effects of buoyancy on the evolution of geophysical boundary layers. *J. Geophys. Res.*, **97**, 15 513–15 527.
- Blanke, B., and P. Delecluse, 1993: Variability of the tropical Atlantic Ocean simulated by the general circulation model with two different mixed layer physics. *J. Phys. Oceanogr.*, **23**, 1363–1388.
- Burchard, H., and H. Baumert, 1995: On the performance of a mixed-layer model based on the $\kappa-\epsilon$ turbulence closure. *J. Geophys. Res.*, **100**, 8523–8540.
- , and K. Bolding, 2001: Comparative analysis of four second-moment turbulence closure models for the oceanic mixed layer. *J. Phys. Oceanogr.*, in press.
- Canuto, V. M., 1992: Turbulent Convection with overshooting: Reynolds Stress Approach. *Ap. J.*, **392**, 218–232.
- , 1994: Large eddy simulation of turbulence: A subgrid model including shear, vorticity, rotation and buoyancy. *Ap. J.*, **428**, 729–752.
- , and —, 1996b: A dynamical model for turbulence: I. General formalism. *Phys. Fluids*, **8**, 587–598.
- , and Y. Cheng, 1997: Determination of the Smagorinsky–Lilly constant C_s . *Phys. Fluids*, **9**, 1368–1378.
- , and M. S. Dubovikov, 1997a: A dynamical model for turbulence: IV. Buoyancy driven flows. *Phys. Fluids*, **9**, 2118–2131.
- , and —, 1997b: A dynamical model for turbulence: V. The effect of rotation. *Phys. Fluids*, **9**, 2132–2140.
- , F. Minotti, C. Ronchi, M. Ypma, and O. Zeman, 1994: Second-order closure PBL model with new third-order moments: Comparison with LES data. *J. Atmos. Sci.*, **51**, 1605–1618.
- Cheng, Y., and V. M. Canuto, 1994: Stably stratified turbulence: A new model for the energy dissipation length scale. *J. Atmos. Sci.*, **51**, 2384–2396.
- Chou, P. Y., 1940: On an extension of Reynolds method of finding apparent stresses and the nature of turbulence. *Chin. J. Phys.*, **4**, 1–33.
- , 1945: On velocity correlations and the solutions of the equations of the turbulent fluctuations. *Quart. Appl. Math.*, **3**, 38–54.

- D'Alessio, S. J. D., K. Abdella, and N. A. McFarlane, 1998: A new second-order turbulence scheme for modeling the ocean mixed layer. *J. Phys. Oceanogr.*, **28**, 1624–1641.
- Davis, R. E., 1994: Diapycnal mixing in the ocean: The Osborn–Cox model. *J. Phys. Oceanogr.*, **24**, 2560–2576.
- Deardorff, J. W., 1980: Stratocumulus capped mixed layer derived from a three dimensional model. *Bound.-Layer Meteor.*, **18**, 495–527.
- Galperin, B., L. H. Khanta, S. Hassid, and A. Rosati, 1988: A quasi-equilibrium turbulent energy model for geophysical flows. *J. Atmos. Sci.*, **45**, 55–62.
- Gargett, A. E., 1989: Ocean turbulence. *Annu. Rev. Fluid Mech.*, **21**, 419–451.
- , and T. R. Osborn, 1981: Small scale shear measurements during the fine and microstructure experiment (FAME). *J. Geophys. Res.*, **86**, 1929–1944.
- , P. J. Hendricks, T. B. Sanford, T. R. Osborn, and A. J. Williams, 1981: A composite spectrum of vertical shear in the upper ocean. *J. Phys. Oceanogr.*, **11**, 1258–1271.
- Gaspar, P., Y. Gregoris, and J. M. Lefevre, 1990: A simple eddy kinetic energy model for simulations of the oceanic vertical mixing: Test at station Papa and long-term upper ocean study site. *J. Geophys. Res.*, **95**, 16 179–16 193.
- Gatski, T. B., S. Sarkar, and C. G. Speziale, Eds., 1992: *Studies in Turbulence*. Springer-Verlag, 602 pp.
- Gent, P. R., and J. C. McWilliams, 1990: Isopycnal mixing in ocean circulation models. *J. Phys. Oceanogr.*, **20**, 150–155.
- Gerz, T., U. Schumann, and S. E. Elghobashi, 1989: Direct numerical simulation of stratified, homogenous turbulent shear flows. *J. Fluid Mech.*, **220**, 563–594.
- Hassid, S., and B. Galperin, 1983: A turbulent energy model for geophysical flows. *Bound.-Layer Meteor.*, **26**, 397–412.
- Howard, L. N., 1961: Note on a paper by J. W. Miles. *J. Fluid Mech.*, **10**, 509–512.
- Kantha, L., and C. A. Clayson, 1994: An improved mixed layer model for geophysical applications. *J. Geophys. Res.*, **99** (C12), 25 235–25 266.
- Large, W. G., J. C. McWilliams, and S. C. Doney, 1994: Oceanic vertical mixing: A review and a model with non-local boundary layer parameterization. *Rev. Geophys.*, **32**, 363–403.
- , G. Danabasoglu, S. C. Doney, and J. C. McWilliams, 1997: Sensitivity to surface forcing and boundary layer mixing in a global ocean model: Annual-mean climatology. *J. Phys. Oceanogr.*, **27**, 2418–2447.
- Launder, B. E., G. J. Reece, and W. Rodi, 1975: Progress in the development of a Reynolds stress turbulent closure. *J. Fluid Mech.*, **68**, 537–566.
- Ledwell, J. R., A. J. Watson, and C. Law, 1993: Evidence for slow mixing across pycloine from open-ocean tracer experiment. *Nature*, **364**, 701–703.
- Levitus, S., and T. P. Boyer, 1994: *World Ocean Atlas 1994*. Vol. 4: *Temperature*, NOAA Atlas NESDIS 4, 129 pp.
- , R. Burgett, and T. P. Boyer, 1994: *World Ocean Atlas 1994*. Vol. 3: *Salinity*, NOAA Atlas NESDIS 3, 111 pp.
- Lumley, J. L., 1978: Computational modeling of turbulent flows. *Adv. Appl. Mech.*, **18**, 123–176.
- , and B. Khajeh-Nouri, 1974: Computational modeling of turbulent transport. *Advances in Geophysics*, Vol. 18A, 169–192.
- Ma, C. C., C. R. Mechoso, A. Arakawa, and J. D. Ferrara, 1994: Sensitivity of a coupled ocean–atmosphere model to physical parameterizations. *J. Climate*, **7**, 1883–1896.
- Maderich, V. S., O. M. Kononov, and S. I. Konstantinov, 1995: Mixing efficiency and processes of restratification in a stably stratified medium. *Mixing in Geophysical Flows*, J. M. Redondo and O. Metais, Eds., International Center for Numerical Methods in Engineering, 393–401.
- Martin, P. J., 1985: Simulation of the mixed layer at OWS November and Papa with several models. *J. Geophys. Res.*, **90** (C1), 903–916.
- Mellor, G. L., 1989: Retrospect on oceanic boundary layer modeling and second moment closure. *Parameterization of Small Scale Processes, Proc. Hawaiian Winter Workshop*, University of Hawaii, 251–272.
- , and T. Yamada, 1982: Development of a turbulence closure model for geophysical fluid problems. *Rev. Geophys. Space Phys.*, **20**, 85–875.
- Miles, J. W., 1961: On the stability of heterogeneous shear flows. *J. Fluid Mech.*, **10**, 496–508.
- Moeng, C.-H., and J. C. Wyngaard, 1989: Evaluation of turbulent transport and dissipation closures in second-order modeling. *J. Atmos. Sci.*, **46**, 2311–2330.
- Monin, A. S., and A. M. Yaglom, 1971: *Statistical Fluid Mechanics*. Vols. 1 and 2. The MIT Press, 769 pp.
- Moum, A. S., 1989: Measuring turbulent fluxes in the ocean. The quest for K_p . *Parameterization of Small Scale Processes, Proc. Hawaiian Winter Workshop*, University of Hawaii, 145–156.
- Munk, W. H., 1966: Abyssal recipes. *Deep-Sea Res.*, **13**, 707–730.
- NCAR Oceanography Section, 1996: The NCAR CSM Ocean Model. NCAR Tech. Note NCAR/TN-423+STR.
- Oakey, N. S., 1982: Determination of the rate of dissipation of turbulent energy from simultaneous temperature and velocity shear microstructure measurements. *J. Phys. Oceanogr.*, **12**, 256–271.
- Osborne, T. R., 1980: Estimates of the local rate of vertical diffusion from dissipation measurements. *J. Phys. Oceanogr.*, **10**, 83–89.
- Pope, S. B., 1975: A more general effective viscosity hypothesis. *J. Fluid Mech.*, **72**, 331–340.
- Rodi, W., 1976: A new algebraic relation for calculating the Reynolds stresses. *Z. Angew. Math. Mech.*, **56**, T219–T221.
- Rosati, A., and K. Miyakoda, 1988: A general circulation model for upper ocean simulation. *J. Phys. Oceanogr.*, **18**, 1601–1626.
- Schumann, U., 1991: Subgrid length-scales for LES of stratified turbulence. *Theor. Comput. Fluid Dyn.*, **2**, 279–290.
- Shih, T. S., and A. Shabbir, 1992: Advances in modeling the pressure correlation terms in the second moment equations. *Studies in Turbulence*, T. B. Gatski, S. Sarkar, and C. G. Speziale, Eds., Springer-Verlag, 91–128.
- Thorpe, S. A., 1977: Turbulence and mixing in a Scottish loch. *Philos. Trans. Roy. Soc. London*, **286A**, 125–181.
- Toole, J. M., K. L. Polzin, and R. W. Schmitt, 1994: Estimates of diapycnal mixing in the abyssal ocean. *Science*, **264**, 1120–1123.
- Wang, D., W. G. Large, and J. C. McWilliams, 1996: Large eddy simulation of the equatorial ocean boundary layer: Diurnal cycle, eddy viscosity and horizontal rotation. *J. Geophys. Res.*, **101** (C2), 3649–3662.
- Webster, C. A. G., 1964: An experimental study of turbulence in a density stratified shear flow. *J. Fluid Mech.*, **19**, 221–245.
- Wuest, A., D. C. van Senden, J. Imberger, G. Piepke, and M. Gloor, 1996: Comparison of diapycnal diffusivity measured by tracer and microstructure techniques. *Dyn. Atmos. Oceans*, **24**, 27–39.